We are IntechOpen, the world's leading publisher of Open Access books Built by scientists, for scientists

4,800
Open access books available

122,000
International authors and editors

135M
Downloads

Our authors are among the

154
Countries delivered to

TOP 1%
most cited scientists

12.2%
Contributors from top 500 universities

CLARIVATE ANALYTICS BOOK CITATION INDEX INDEXED

WEB OF SCIENCE™

Selection of our books indexed in the Book Citation Index in Web of Science™ Core Collection (BKCI)

Interested in publishing with us?
Contact book.department@intechopen.com

Numbers displayed above are based on latest data collected.
For more information visit www.intechopen.com

4

Ubiquitous Piezoelectric Sensor Network (UPSN)-Based Concrete Curing Monitoring for u-Construction

Seunghee Park and Dong-Jin Kim
Department of Civil and Environmental Engineering/u-City Design and EngineeringSungkyunkwan University
Cheoncheon-dong Jangan-gu Suwon
Republic of Korea

1. Introduction

Recently, there has been increasing demand for high-rise buildings or wide-span bridges. These structures are constructed with a mount of mass concrete. However, the concrete might be susceptible to brittle fracture if the curing process is inadequate. Therefore, to prevent this drawback, it is essential to predict the strength development of concrete during the curing process. In addition, real-time monitoring of the curing strength is important for reducing the construction time and cost because it can determine the appropriate curing time to achieve sufficient strength to progress to the next phase safely. The in-situ strength of concrete structures can be determined with a high precision by performing the strength testing and/or material analysis on core samples removed from the structure (Irie et al., 2008). However, this method might destroy the concrete structure. Therefore, a range of methods based on the thermal, acoustical, electrical, magnetic, optical, radiographic, and mechanical properties of the test materials have been developed to monitor the strength development without damaging the host structures (ACI Committee 228, 2003; Lamind and Pielert, 2006; Metha and Monterio, 2005). These methods typically measure certain properties of concrete from which the strength and/or elastic constants can be estimated. Among these techniques, several methods using a Schmidt hammer or an integrated temperature have been normally used. However, these are unsuitable for use at construction sites because they do not allow real-time monitoring of the curing process of concrete structures at inaccessible places.

The recent advent of smart materials, particularly piezoelectric materials, can provide a solution for the real-time monitoring for strength development. Electromechanical impedance techniques that employ piezoelectric materials have emerged as a potential tool for the implementation of a built-in monitoring system for civil infrastructures (Park G. et al., 2000, 2003; Park S. et al. 2005, 2006, 2011). This technique utilizes high-frequency structural excitation, which is typically > 20 kHz from surface-bonded PZT (Lead-Zirconate-Titanate) patches, to sensitively monitor the changes in the mechanical impedance of the test structures. Furthermore, the recent advances in online monitoring, including actuation and sensing, on-board computing, and radio-frequency (RF) telemetry, have improved the

accessibility of the impedance method for in-field measurements. Lynch et al. (2004) designed a wireless active sensing unit to monitor civil structures, which was constructed of off-the-shelf components and had the ability to command active sensors and actuators from a computational core combined with wireless transmission and sensing circuits, embedded algorithm to process the acquired data, and structural status broadcasting. Grisso and Inman (2005) designed a DSP (Digital Signal Processor) based prototype to provide wireless assessment of thermal protection systems. It was able to directly detect damages by analyzing variations of the electrical impedance of PZT sensors bonded to the structure. The obtained impedance signals were compared with the pre-stored baseline and a statistical damage index was calculated. Mascarenas et al. (2007) proposed a wireless sensor node which consists of a miniaturized impedance measuring chip, a microprocessor, and a radio-frequency identification (RFID) module. Low cost impedance measuring chip actuated the structure through a PZT and measured the structural impedance response, and RFID module delivered the diagnostic result to a base station. Park S. et al. (2009) improved the wireless sensor node of Mascarenas et al. (2007) by adding two multiplexer IC chips for 16 channels for the cases of multiple sensors in a small region and by embedding signal processing algorithms in the microcontroller unit (MCU) for both structural damage identification and sensor self-diagnosis. Research groups at Los Alamos National Lab recently developed a compact impedance-based wireless sensing device (WID3) for low power operation (Overly et al. 2007, 2008), which requires around 60 mW of power to operate. Here, a wake-up capability was combined for low power operation. Taylor et al. (2009a, b) extended the capability of the WID3 by implementing a module with low-frequency A/D and D/A converters to measure low-frequency vibration data for multiple SHM techniques. It is wirelessly triggered by a mobile agent for use in the mobile-host-based wireless sensing network. Min et al. (2010) developed a multi-functional wireless sensor node integrating piezoelectric actuating, sensing, signal processing, temperature compensating, and energy harvesting modules.

In this context, this study presents a series of efforts to confirm the applicability of the electromechanical impedance technique using both wired and wireless systems for online monitoring on the strength-development during the curing process of concrete.

2. Electromechanical impedance based concrete strength estimation

As already described, in order to manage effectively the construction process of the concrete structures, online monitoring of the concrete strength-development is strongly required. To end this, this study employs the electromechanical impedance-based structural health monitoring (SHM) methodology because the electromechanical impedance can represent the mechanical properties of a host structure. The strength variation developed during the curing process can be observed throughout the electromechanical impedance measurements.

2.1 Strength development due to concrete curing process

Concrete achieves its strength through a hydraulic process known as hydration. With the addition of the correct amount of water, the cement gels into a paste that glues sand and aggregates together to form hardened concrete. The curing of concrete involves maintaining a proper moisture vapor transmission rate (2% mvtr) immediately after concrete placement

as well as throughout the ensuing period of approximately 28 days. Fig. 1 shows a typical strength development curve (Shariq et al., 2010).

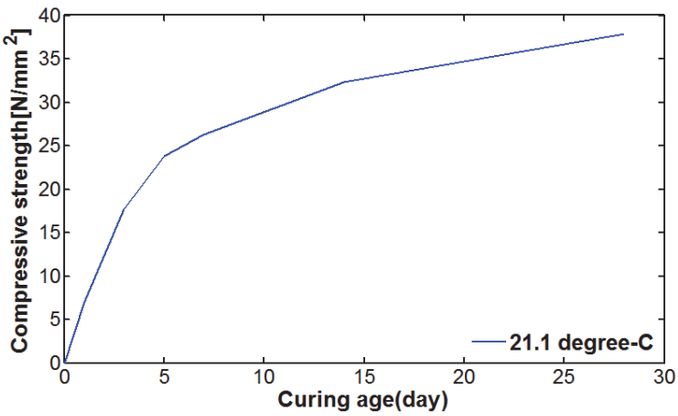

Fig. 1. Typical Strength Development Curve

2.2 Electromechanical impedance modeling

The electromechanical impedance-based SHM techniques have been developed as a promising tool for real-time structural damage assessment on critical members of large structural systems (Park G. et al., 2003, Koo et al., 2009, Taylor et al., 2009a, 2009b, Mascarenas et al., 2009). They make use of piezoelectric sensors such as piezoceramic (PZT) and macro-fiber composite (MFC) patches, which form a collocated sensor and actuator, often referred to as a self-sensing actuator (Giurgiutiu, 2007). The basis of this active sensing technology is the energy transfer between the actuator and the host mechanical system. If a PZT attached on a structure is driven with a sinusoidal voltage, it causes the local area of the structure to vibrate (the converse piezoelectric effect). And the structural response causes an electrical response in the PZT (the direct piezoelectric effect). Liang et al. (1996) first proposed a one-dimensional analytical model of this setup as in Fig. 2, and showed that the electrical admittance (inverse of the electrical impedance), Y(ω), of a PZT is directly correlated to the local mechanical impedance of the host structure, Zs(ω), and that of a PZT patch, Za(ω), in most applications as

$$Y(\omega) = G(\omega) + jB(\omega) = j\omega C\left(1 - \kappa_{31}^2 \frac{Z_s(\omega)}{Z_s(\omega) + Z_a(\omega)}\right) \quad (1)$$

where G is the conductance (real part); B is the susceptance (imaginary part); C is the zero-load capacitance of a PZT; and κ31 is the electromechanical coupling coefficient of a PZT. Given that the mechanical impedance and the material properties of the PZT stay constant, the equation shows that a change in the structure's mechanical impedance directly results in a change in the electrical impedance measured by the PZT. Since damages cause a change in the structure's local mass, stiffness, or damping properties and consequently its mechanical impedance, the structure's mechanical integrity can be assessed by monitoring the PZT's electrical impedance. It should be noted that the admittance function, Y(ω), is a complex number. Bhalla et al. (2002) demonstrated that the real part of the measured admittance is more sensitively changed due to the structural damage condition as compared to the

imaginary part. On the other hand, Park G. et al. (2006) found out that the imaginary part can be more effectively used for piezoelectric sensor self-diagnosis.

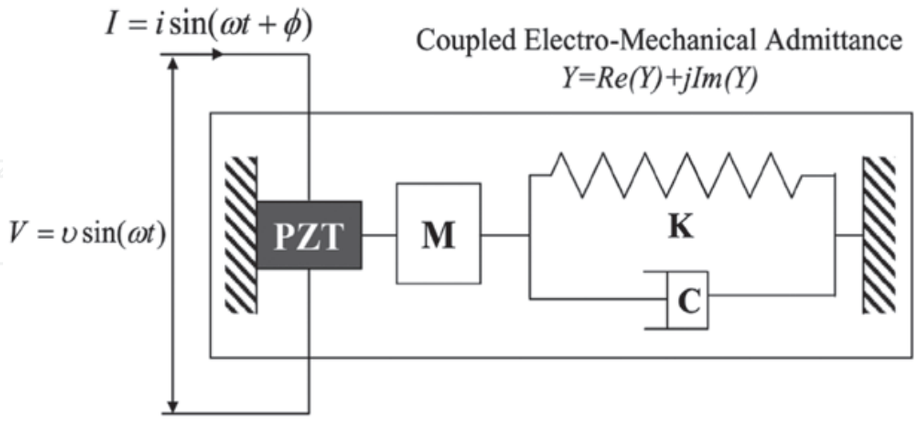

Fig. 2. 1-D Model used to derive electromechanical admittance of a PZT bonded to a structure (Liang et al. 1996)

2.3 Self-sensing based wired impedance measurement method

In this study, impedance measurement systems are based on a self-sensing technique, as shown in Fig. 3. A self-sensing circuit as described in Fig. 3 is suitable for use in cast-in-site concrete because it is inexpensive and has sufficient accuracy to measure the development of strength, even though the impedance signal is less accurate than other impedance measurement methods. The self-sensing circuit board consists of a single PZT patch, and a voltage divider, such as a resister or capacitor to acquire the output voltage.

The impedance is measured in three steps based on the self-sensing circuit as follows: (1) the input voltage (V_i) generated from an arbitrary waveform generator (AWG) is applied to the free surface of the PZT sensor; (2) the output voltage from the self-sensing circuit (V_o) is measured using a digitizer (DIG); and (3) the admittance, which is the inverse of impedance, is derived from the input voltage, output voltage, and reference capacitance (C_r). The output voltage from the self-sensing circuit consists of the input voltage and mechanical response of the structure (V_r). Although the amplitude of the mechanical responses of the structure is small enough to ignore, the output voltage is dominated by the input voltage and can be approximated as follows (Lee and Sohn, 2006)

$$V_o(t) = \frac{C_p}{C_p + C_r}\left[V_i(t) + V_p(t)\right] \simeq \frac{C_p}{C_p + C_r}V_i(t) \tag{2}$$

where C_p is the PZT capacitance and C_r is the reference capacitance of the self-sensing circuit. From Eq. (2), the impedance of structure (Z) is derived as follows:

$$Z(\omega) = \frac{V_p(\omega)}{I(\omega)} = [iwC_p]^{-1} \simeq \left[i\omega C_r\left(\frac{V_o(\omega)}{V_i(\omega) - V_o(\omega)}\right)\right]^{-1} \tag{3}$$

Thus, the impedance explained at Eq. (1) could be measured by Eq. (3) using the self-sensing circuit displayed in Fig. 3.

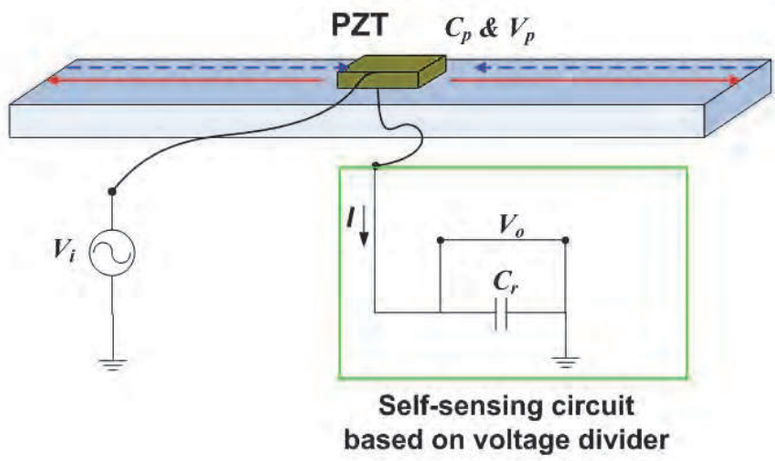

Fig. 3. Schematic diagram of a self-sensing circuit

3. Development of wireless impedance sensor nodes

The recent advances in wireless online monitoring integrating actuation and sensing, on-board computing, and radio-frequency (RF) telemetry improved the accessibility of the electromechanical impedance method for in-field measurements. In this study, the multi-functional wireless sensor node developed by Min et al. (2010) was utilized.

3.1 Subsystems of wireless impedance sensor nodes

To measure the electromechanical impedances, impedance analyzers such as HP4294A are conventionally used. However, they are not quite suitable for field applications to online SHM because they are bulky (approximately 25 kg) and expensive (approximately 40,000 USD). Thus, research on the impedance based SHM technique trends toward development of self-contained sensors and wireless active sensor nodes with all required functions including actuating/sensing, data processing, damage assessments and sensor self-diagnostics on the sensor board as well as power management with energy harvesters. Recently, Analog Devices© developed an integrated impedance converters, AD5933 (www.analog.com). It is equipped with a 12-bit analog-to-digital converter (ADC), a digital-to-analog converter (DAC) and a discrete Fourier transform (DFT) functionality. The frequency generator allows an external complex impedance with range of 100 Ω to 10MΩ to be excited with a known frequency of up to 100 kHz. AD5933 is just of a penny size, thus it provides a solution for self-contained miniaturized impedance measuring. Therefore, AD5933 has been used as a core component in developing a wireless impedance sensor node for SHM applications (Mascarenas et al. 2007, 2009, Overly et al. 2007, 2008, Taylor et al. 2009a, b, Park S. et al. 2009, Min et al. 2010). The wireless sensor node, proposed in this study, has extended the previous researches for multifunctional and environment-friendly uses in the impedance-based SHM (Mascarenas et al. 2007, Park S. et al. 2009). It was designed by adding: (1) optimal arrangement of each chip for low power consumption, (2) energy harvester equipped with solar panels, (3) peer-to-peer communication by using a RF transceiver of CC2420, which enables to construct the ubiquitous sensor network, (4) internal algorithms for operations, which are optimized by using microcontroller-dependent

instruction codes to boost the sensor node's capability and (5) miniaturized hardware system fabricated as a printed circuit board (PCB) for a high quality prototype and enclosed by waterproof plastic box for applications to real structures. The proposed wireless sensor node is composed of four functional subsystems: (1) sensing interface, (2) computational core, (3) wireless transceiver and (4) power supply. The "sensing interface" includes an interface to which a piezoelectric sensor and a temperature sensor can be connected, and an impedance chip (AD5933) for exciting a piezoelectric sensor and measuring the impedance signals. Here, NTC (Negative Temperature Coefficient) disc thermistor is equipped for temperature sensing on the structure near a piezoelectric sensor. It is a low-cost and small-size resistance type device, and is suitable for temperature ranges from -20 ^{o}C to +120 ^{o}C with reference resistance of 10 kΩ at 25 ^{o}C. The "computational core" consists of a microcontroller and a serial flash memory for computational tasks and system operations with various embedded algorithms. Through embedding technologies in microcontroller, the wireless traffic can be reduced and the survival rate of transmitted data can be increased. In this sensor node, ATmega128L is adopted because it is one of high performance and low power 8-bit microcontrollers, and has 128 kilobytes of in-system self-programmable flash program memory (www.atmel.com). The "wireless transceiver" is an integral component of the wireless system, which is composed of a RF transceiver (CC2420), a balun transformer, and an antenna to communicate with a base station (Kmote-B radio module) and/or other wireless sensor nodes and to broadcast the structural condition. CC2420 is a single chip 2.4 GHz IEEE 802.15.4 compliant RF transceiver designed for low-power and low-voltage wireless applications (www.ti.com). It provides a low-cost and highly integrated solution for robust wireless communication and extensive hardware support for packet handling, data buffering and burst transmission. These features reduce the load on the host controller and allow CC2420 to interface low-cost microcontrollers. The sensor node can be operated by one of three type "power supply" systems: 5 V AC-plug DC adapter, 3.6-7.2 V battery, or 5 V solar power system. The power can be monitored on the microcontroller using a general ADC, which transforms the analog signals acquired from batteries to the digital signals. For stable power supply to the sensor node during operations, LDO (Low-dropout regulator) is mounted for providing a fixed 3.3 V reference output to the sensor node. Solar power system for energy harvesting consists of single crystalline silicon solar cells (120 × 60 mm2) to generate the maximum power for its size, two AA Ni- MH rechargeable batteries to stand high temperature and overcharging under sunlight and to last up to 1000 charge/discharge cycles, and a step-up DC/DC solar controller to protect the appliances and the batteries with over discharge prevention circuit. Fig. 4 shows the impedance sensor node developed in this study and its block diagram, and the features are described in Table 1. The developed impedance sensor node was tested on the several operational conditions to determine the actual in-service power consumption. A multimeter was placed in line on the node's positive voltage terminal. The current draw during each condition was recorded as: 1.3 mA in idle state, 25.8 mA during measurement, 15.2 mA during calculation, and 27.3 mA during transmission, which indicates that the maximum required power is approximately 90 mW with 3.3 V.

It is slightly larger than the required power of 60 mW by Overly et al. (2008), which may be caused by additionally equipped NTC thermistor for temperature sensing, three LEDs for informing the node status by twinkling with different colors, and other operation subsystems. The required power may be reduced further with proper use of sleep modes in Overly et al. (2008).

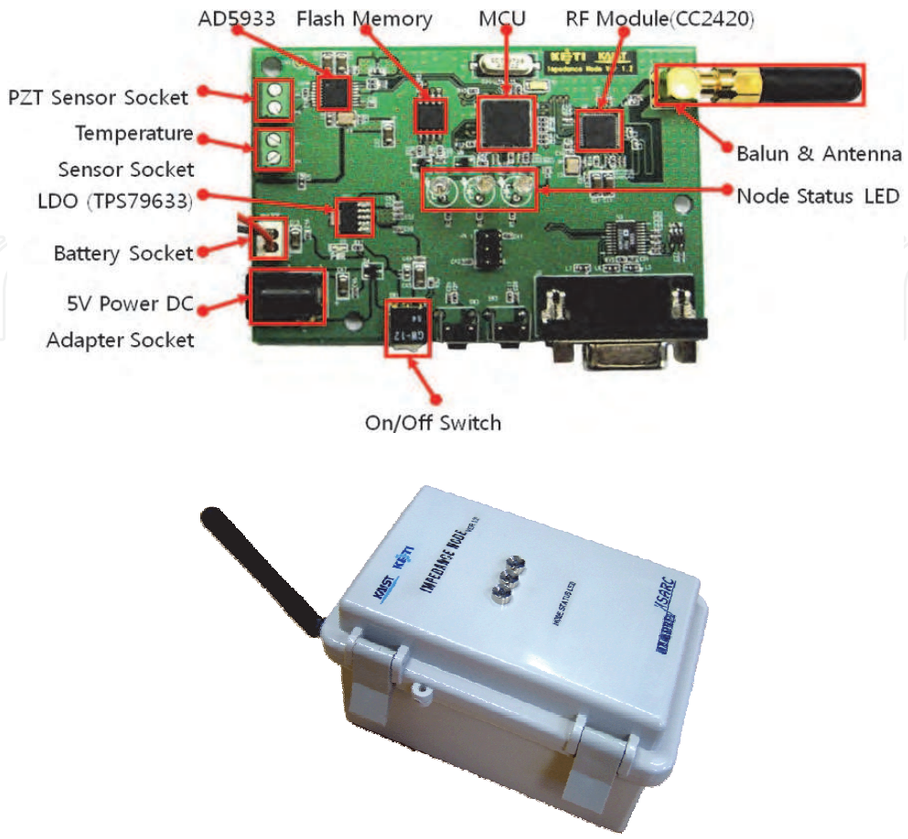

(a) Subsystem and enclosure

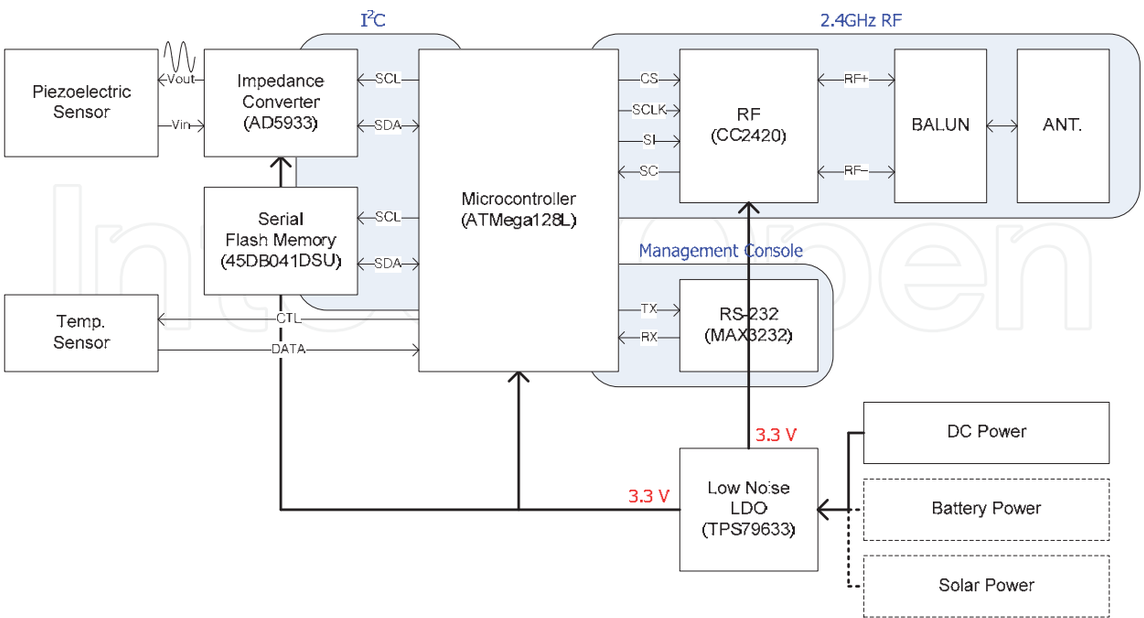

(b) Block diagram

Fig. 4. Proposed wireless impedance sensor node

Output Frequency Range	1 ~ 100 kHz
Output Frequency Resolution	> 1 Hz
Impedance Range	1 kΩ ~ 1 MΩ
Temperature Range	-40 ~ 125 °C
Temperature Resolution	> 0.03 °C
On-Board Processing	Yes (MCU : ATMega128L)
Operating Frequency	2.4 GHz IEEE 802.15.4 / Zigbee RF Transceiver
Outdoor Transmission Range	150 m
Power Supply Options	• 5V AC-plug DC Adapter • Commercial batteries (3.6-7.2V) • 2AA Ni-MH rechargeable battery with Solar Panels (3V)
Feature	150 x 100 x 70 (mm) ; 310 (g)

Table 1. Features of the proposed wireless impedance sensor node

3.2 Data control and on-board data analysis

TinyOS is the most typical open-source operating system designed for wireless embedded sensor networks. It features a component-based architecture which enables rapid innovation and implementation while minimizing code size as required by the severe memory constraints inherent in sensor networks.

The proposed sensor node is based on TinyOS for system operation. On the other hand, the server is controlled by users through MATLAB® software, which is a high-level language and interactive environment to perform computationally intensive tasks faster than traditional programming languages such as C, C++, or FORTRAN, and includes a number of mathematical functions including Fourier analysis, filtering, signal processing and serial communications. Moreover, it provides GUI (graphical user interface) development environment, from which the user can easily change the control variables and monitor the wirelessly transmitted raw and/or processed data, temperature and node status such as battery condition. The serial communication is established between a server and a base station using two service daemons, which are cross-complied using Cygwin. These daemons provide a Linux-like environment for Windows, and enable to communicate between MATLAB® (Windows) and base station/sensor node (TinyOS).

For continuous and autonomous SHM using wireless sensor nodes, it is strongly required to construct the embedded data analysis system. More power-efficient wireless SHMs could be achieved, if the measured impedance is analyzed on microcontroller of the sensor node and only the analyzed results Table 1 Features of the proposed wireless impedance sensor node could be wirelessly sent to a base station. Especially, this fact is crucial for self-powered wireless sensor nodes incorporating several kinds of energy harvesters. In the proposed sensor node, multifunctional algorithms are implemented for temperature/power measurement, impedance measurement and analysis engine for both structural damage detection and sensor self-diagnosis, as shown in Fig. 5.

The impedance measurement block consists of the TWI library, AD5933 control library and the default sweep function (512 points) library. Using raw data from the impedance

measurement block, the embedded analysis engine optionally performs the analysis for structural damage detection and sensor self-diagnosis. Two algorithms are embedded on the microcontroller for the structural status monitoring: the RMSD metric and the temperature compensated CC metric calculated by EFS method. Sensor self-diagnosis is simply carried out calculating the slope of the imaginary part of admittance. Here, the baseline impedance is stored at the serial flash memory. Depending on input arguments, the users can get raw or processed data from the designated sensors.

3.3 Self-powered wireless system incorporated with solar cells

Power scavenging enables "place-and-forget" wireless sensor node. Considering that the necessary cost and efforts for battery maintenance and replacement may over-shadow the merits of the wireless SHM system, the ability to scavenge energy from the environment is a quite important and it permits deploying self-powered sensor nodes onto inaccessible locations. Thus, many researchers have shown interest in power scavenging and the related technologies have steeply grown. Especially, the solar power is most often used, which is produced by collecting sunlight and converting it into electricity.

This is done by using solar panels, which are large flat panels made up of many individual solar cells. In this study, a solar power system for operating a wireless sensor node is designed with single crystalline silicon solar cells (120 × 60 mm2), two AA Ni-MH rechargeable batteries (1.2 V × 2ea), and a step-up DC/DC solar controller, considering one-time measurement per day. A step-up DC/DC solar controller offers 4.8 V reference output from a lowered battery voltage of more than 2 V.

This solar power system provides maximum 750 mW, which may be enough to operate the developed sensor node of 90 mW. If the larger power is needed for more frequent measurements per day, the recharging capacity of the solar power system may be increased by using higher-efficient and bigger size solar panels and higher-voltage batteries. To validate the ability of the solar power system, a simple experiment has been carried out on an aluminum plate as shown in Fig. 6. A macro-fiber composite (MFC) patch of 47 × 25 × 0.267 mm3 (2814P1 Type; Smart Material©) was surface-bonded to the aluminum specimen of 50 × 1,000 × 4 mm3. The MFC is a relatively new type of PZT transducer that exhibit superior ruggedness and conformability compared to traditional piezoceramic wafers. At the beginning, the batteries were fully recharged by an electric battery charger. Then, the experiment started at 00:00 am on 6 September, 2009. Raw impedance signals and the processed structural damage detection results were wirelessly transmitted to a base station at every 10:00 am for five days. The weather condition was changed in five days as follows: sunny (19.6-31.1 ^{o}C; cloud 0.8), mostly cloudy (20.9-27.9 ^{o}C; cloud 7.6), partly cloudy (21.0-29.8 ^{o}C; cloud 5.3), partly cloudy (17.9- 28.6 ^{o}C; cloud 4.3), and partly cloudy (14.5-28.5 ^{o}C; cloud 6.8). Fig. 7 shows the voltage level in two AA rechargeable batteries during five days, which was measured every one hour.

Although the voltage steeply declined during the measurement of impedances and on-board calculation of damage index, it was almost fully recovered in one hour under sun light.

It may indicate that it is able to operate the sensor node several times per day. The recharged voltage remained on stable condition under sun light, but it decreased at 0.005 V/hour at night. When cloudy, the solar cells could not be recharged due to the lack of sun light, but it shortly returned to stable condition as the sun rose. From the above results, it may be concluded that the solar power system is able to provide a solution for maintenance-

free wireless sensor nodes in spite of sensitive reaction to the environment, which would be complemented by development of the more efficient energy scavenging technologies.

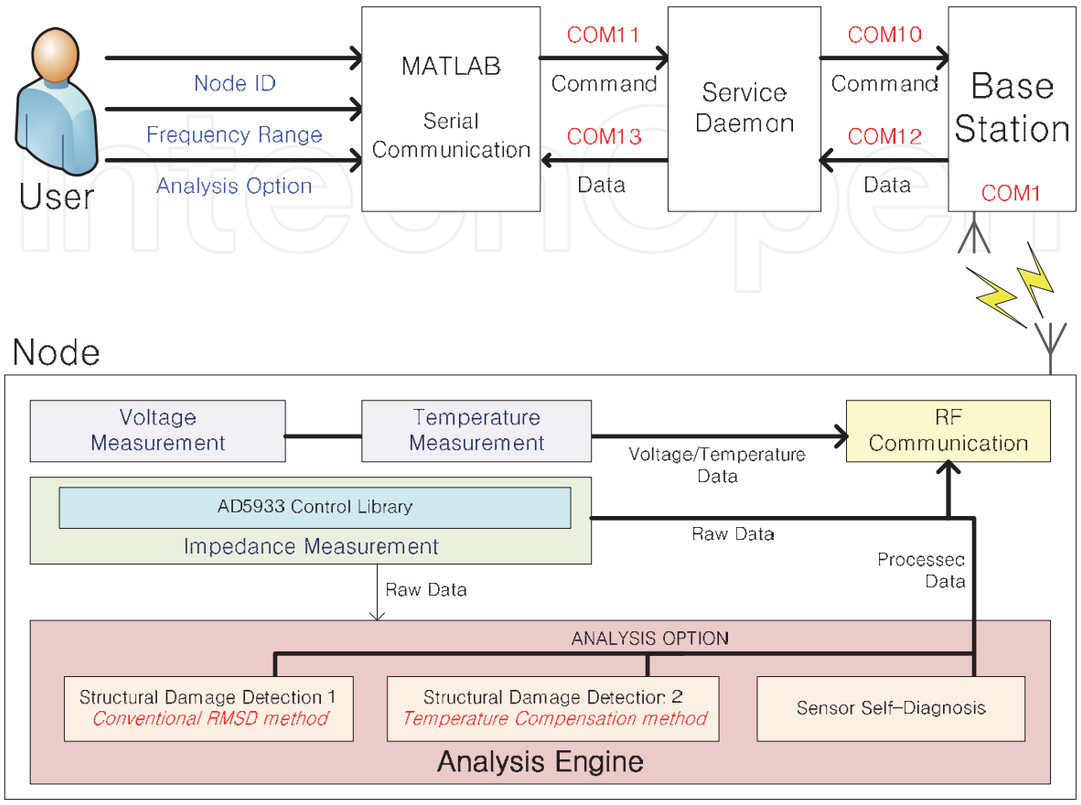

Fig. 5. Overall command/data flow of embedded software

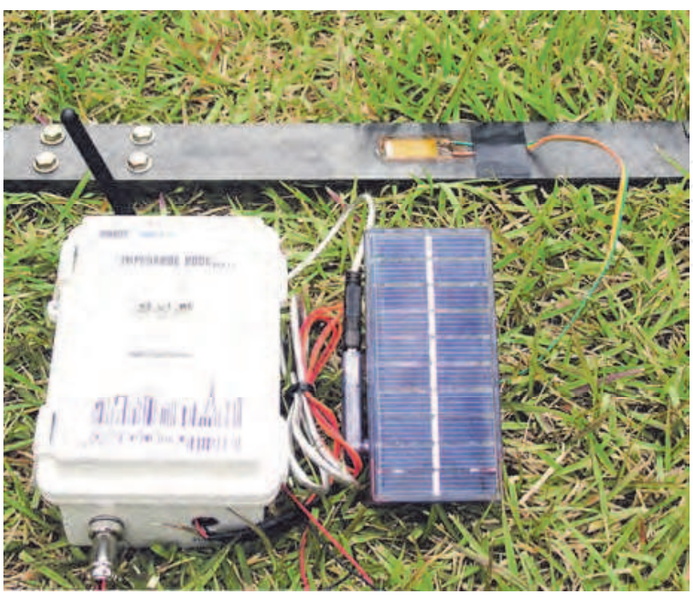

Fig. 6. Sensor node with a solar panel

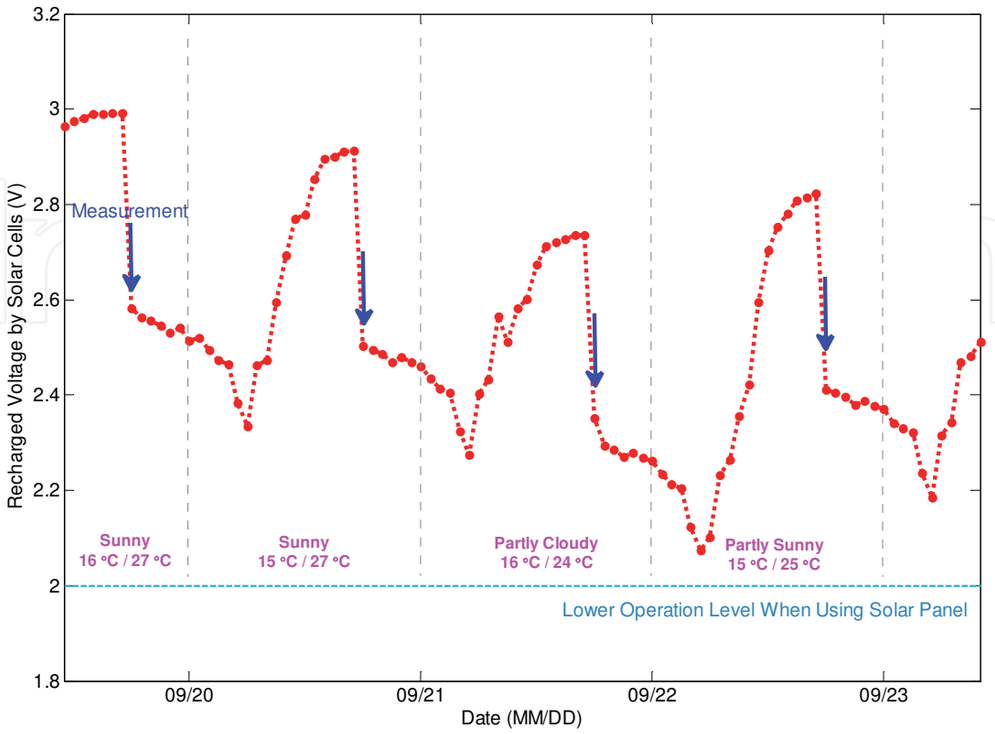

Fig. 7. Voltage monitoring of a wireless SHM system with solar cells

4. Experimental verification

In order to verify the feasibility of the proposed electromechanical impedance technique for online monitoring of the strength developed during the curing process of the concrete structures, a series of experimental studies have been carried out using both wired and wireless systems.

4.1 Experimental setup and test procedure

Two types of concrete cylinders with design strength of 60MPa and 100MPa were prepared to measure the impedance signals during the curing process of concrete, as shown in Fig. 8. The cylinders were developed by isothermal air curing. PZT sensors, 20 mm × 20 mm × 0.508 mm in size, were attached to the concrete cylinders. The PZT sensors were installed on the cylinders in the first 24 hours after casting. Since concrete is a non-conducting material, a conducting copper paste was applied to the specimen before bonding the PZT sensor to the host structure. The PZT patches were bonded to the top center of the cylinder surface, as shown in Fig. 8. The experimental setup for the wired impedance measurement system consisted of cylinders with the PZT sensors, a self-sensing circuit board and a DAQ system (PXI 1042Q, National Instruments Inc.). The DAQ system consisted of an Arbitrary Waveform Generator (AWG), a Digitizer (DIG), embedded controller and data acquisition software (LabVIEW). The wireless system was comprised of the cylinders with the PZT sensors, a wireless sensor node, a RF receiver (KETI), and a laptop computer equipped with data acquisition software (MATLAP), as shown in Fig. 9, 10.

(a) 60MPa Concrete specimen

(b) 100MPa Concrete specimen

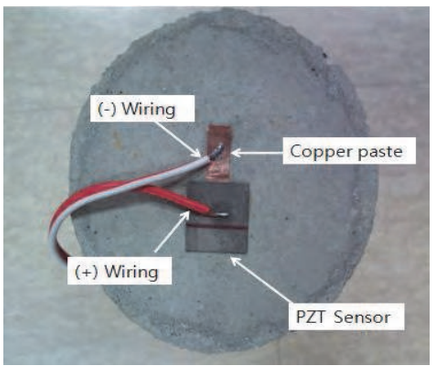

(c) PZT attached concrete specimen

Fig. 8. Test specimen: High Strength Concrete Cylinders

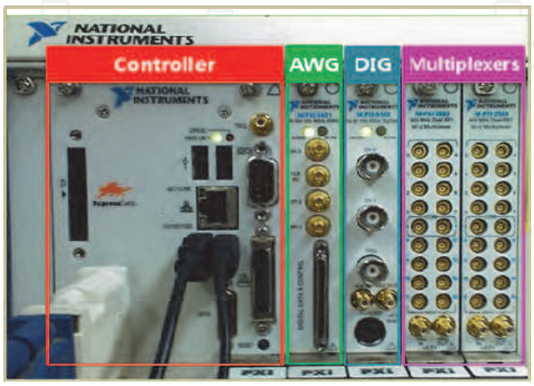

(a) NI-PXI DAQ system

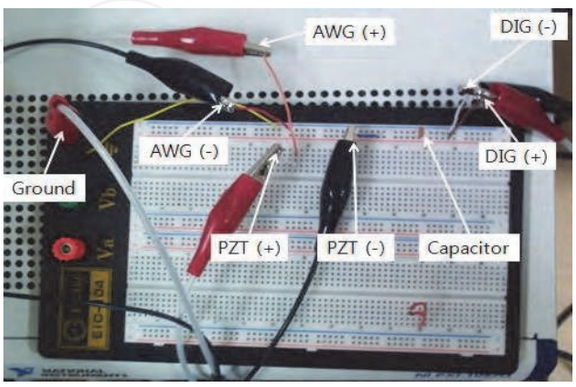

(b) Self-sensing circuit

Fig. 9. Wired impedance measuring system

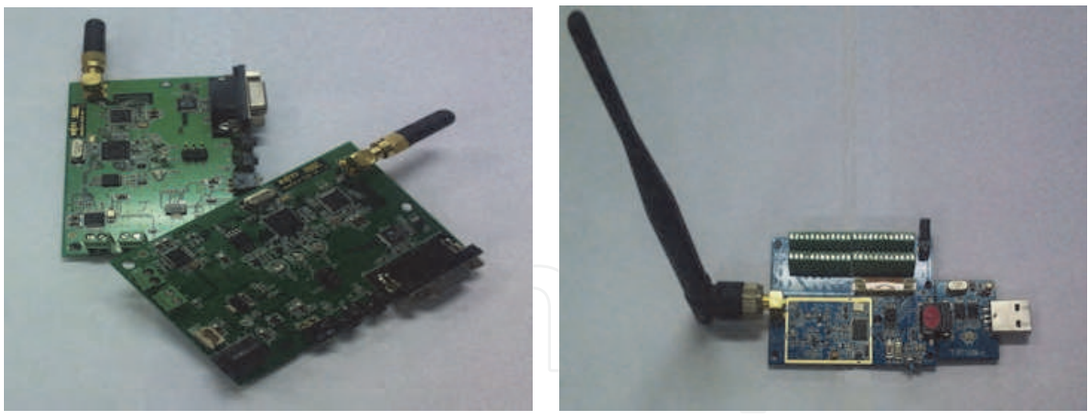

(a) Wireless impednace sensor node (b) RF reciever

Fig. 10. Wireless impedance measuring system

The frequency ranges so the shift in the resonant frequencies could be observed clearly in the measured impedance signals were determined to be 45 kHz ~ 50 kHz for the 60MPa cylinder and 35 kHz ~ 40 kHz for the 100MPa cylinder. The first test was carried out 3 days after mixing because before 3 days, the piezoelectric sensors could not be attached completely. Subsequent tests were performed at 5, 7, 14, 21 and 28 days. In particular, days 3, 7, 14, and 28 are important days in evaluating the in-place compressive strength in the construction codes of many countries. Three cylinders for each group were tested using the wired and wireless systems simultaneously to compare their performance. To improve the signal to noise ratio, the signals were acquired 3 times and averaged.

4.2 Impedance variations due to curing process

The strength of the concrete results from the hydration process of the concrete. During hydration, the mechanical properties of the concrete, such as strength, impedance etc., changed. The impedance technique for monitoring the strength development of concrete employs the change in the mechanical impedance during the hydration process. Figs. 11 and 12 show the measured impedance signals from the wired and wireless systems at six different curing ages. In addition, each dataset was normalized to the maximum value. First, the results from the 60MPa are reported. The resonant frequencies in the impedance signals shifted gradually to the right side with increasing curing age (Fig. 11) due to strength development of the concrete. This confirmed that the impedance technique can be used to monitor the strength development of concrete. In Fig. 12, the impedance data from the 100MPa specimens showed a similar pattern to that obtained from the 60MPa specimens. Although wireless data has some noises, the quantity of the shift in the resonant frequency measured using the wired and wireless system was similar. The noises of wireless data are caused by the resolution problem of wireless sensor node. The frequency resolution can be fixed at a certain level (in this study, that is 1Hz) when NI PXI equipment is used. However, the wireless sensor node can sample with maximum 512 points. In this study, the frequency band of the measured signal is 5kHz with 500 sampling points. Hence, the frequency resolution is 10Hz when the wireless sensor node is used. However, these bumps can be negligible because these cannot affect to the patterns from the curing process. Therefore, the applicability of a wireless impedance measuring system to monitor the curing process of concrete was established.

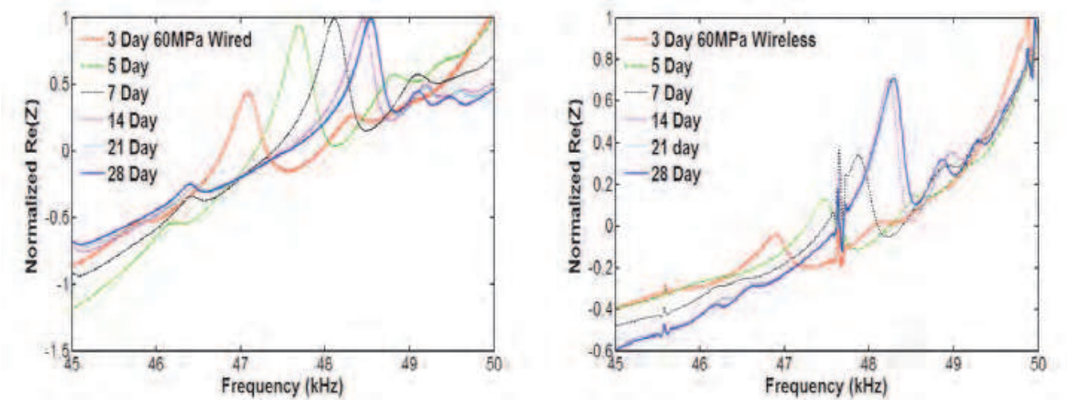

(a) Wired data (b) Wireless data

Fig. 11. Impedance variation measured at 60MPa concrete cylinder

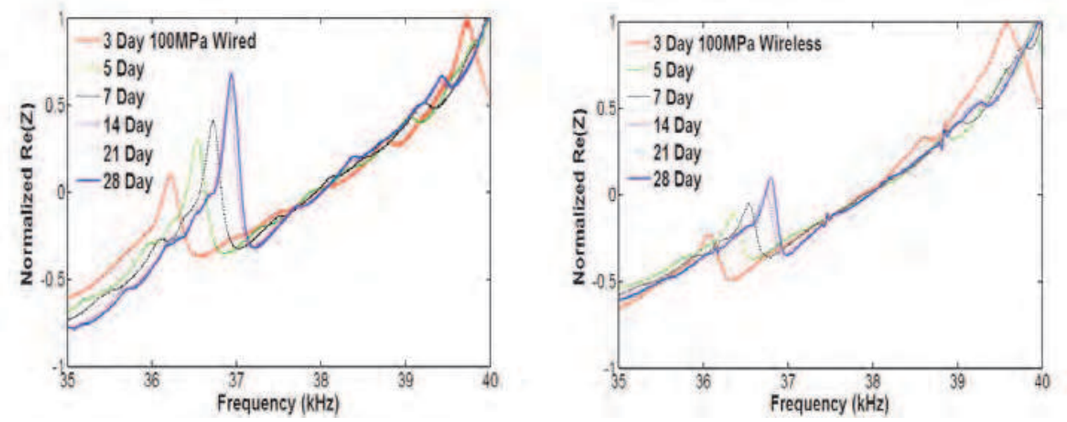

(a) Wired data (b) Wireless data

Fig. 12. Impedance variation measured at 100MPa concrete cylinder

4.3 Signal processing for the impedance variation

Two methods, resonant frequency and cross-correlation coefficient, were applied to examine the trend of the impedance variations more precisely:

4.3.1 Resonant frequency shift

To visualize the curing process of the concrete, the resonant frequency shift (RFS), derived as Eq. (4), at each curing age was plotted, as shown in Fig. 13.

$$RFS = \frac{f_i - f_o}{f_o} \tag{4}$$

where f_i is the current resonant frequency of the impedance data at each measurement day, and f_o is the resonant frequency of the 3rd day measured impedance data as a baseline.

The resonant frequency increased in both cases 60MPa and 100MPa. All the resonant frequency shift data was normalized to the maximum value. As the curing process progressed, the strength of the cylinder increased during the hydration process. Since the resonant frequency is associated with the strength of a concrete cylinder, the resonant frequency in the impedance signals of the cylinder increased with increasing cylinder strength. In addition, the change in resonant frequency measured using the wired system and wireless system were similar in 60MPa and 100MPa. Fig. 1 shows a typical strength development curve of 30MPa at a curing temperature of 21.1 ^{o}C to compare these results with the typical strength development of curing concrete. The changing patterns between the increasing resonant frequency and the development of the compressive strength were similar. Also the RFS of wired and wireless represent similar pattern. Therefore, the RFS of the impedance can be used to monitor the strength development of the concrete.

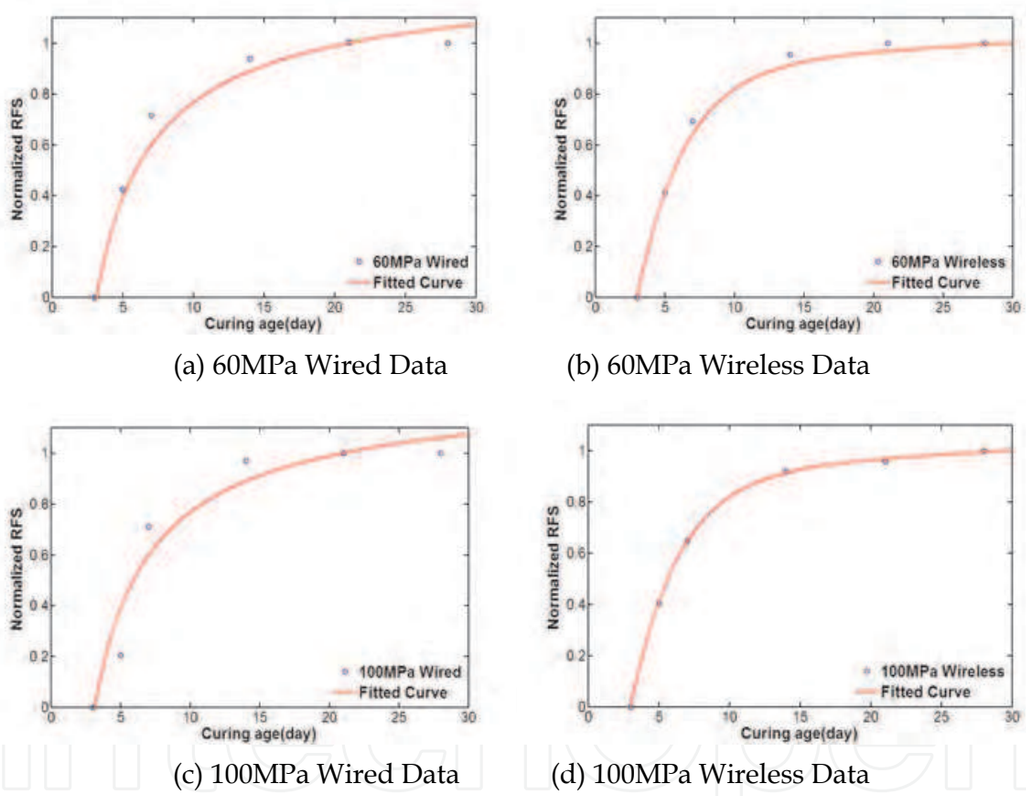

(a) 60MPa Wired Data (b) 60MPa Wireless Data

(c) 100MPa Wired Data (d) 100MPa Wireless Data

Fig. 13. Resonant frequency shift-based estimate of strength development

4.3.2 Cross-correlation coefficient

In addition to the RFS, the cross-correlation coefficient index (1-CC) was calculated to provide quantitative information. The 1-CC values were derived using the following equation:

$$1-CC = 1-\frac{1}{N-1}\frac{\sum_{i=1}^{N}(\mathrm{Re}(Z_{i,0})-\mathrm{Re}(\overline{Z_0}))(\mathrm{Re}(Z_{i,1})-\mathrm{Re}(\overline{Z_1}))}{\sigma_{Z_0}\sigma_{Z_1}} \tag{5}$$

where $Z_{i,0}$ is the impedance function at the baseline (the impedance data of 3rd day), $Z_{i,1}$ is the current impedance at each measured day, and $\sigma_{Z_0}, \sigma_{Z_1}$ are the standard deviations of each dataset, respectively. The data was normalized to the maximum value. Fig. 14 shows the 1-CC data of 60MPa and 100MPa respectively. The 1-CC data shows the same pattern with a commercial strength development curve (Fig. 1). Also, the wired data and wireless data has similar pattern. Therefore, the 1-CC value can provide more reliable quantitative information on strength development.

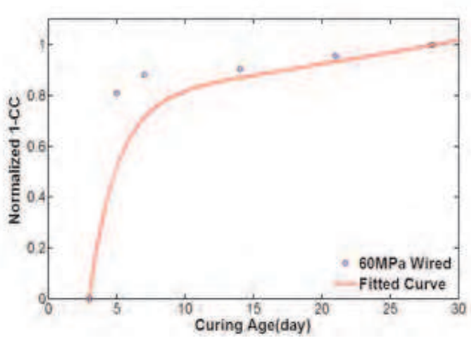

(a) 60MPa Wired Data

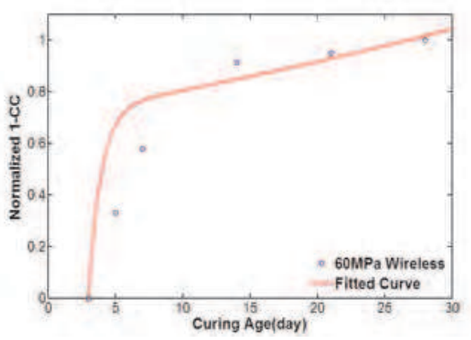

(b) 60MPa Wireless Data

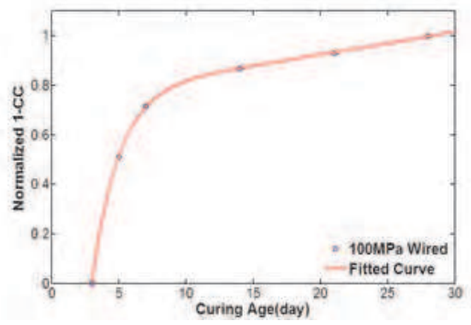

(c) 100MPa Wired Data

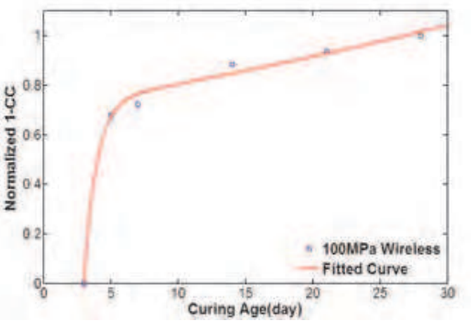

(d) 100MPa Wireless Data

Fig. 14. 1-CC-based estimate of strength development

5. Conclusion

This study evaluated the application of PZT sensors for monitoring the strength development of high strength concrete. The applicability of the conventional impedance measuring technique, which is normally used to detect damage, was extended to monitor the curing process of concrete. The impedance signals were obtained at six different curing ages. The compressive strengths of the test concrete cylinders were also evaluated by considering the resonant frequency variations and cross-correlation coefficient. Based on the experimental results, the resonant frequencies in the impedance signals shifted gradually to the right side with increasing curing time, which confirms the applicability of impedance measurements to monitor the strength development of concrete. The largest deviation of the resonant frequency shift was observed between days 3 and 5, and the change decreased with time. In addition, the 1-CC values increased due to strength development during the curing process. A wireless impedance system showed similar results to that of the wired

impedance system. Therefore, a wireless system that can improve the applicability to a construction site can be used to monitor the strength development of concrete. Consequently, the wireless strength development monitoring system for concrete can be employed comfortably in construction sites. Furthermore, piezoelectric sensors that monitor the strength development can be used for structural health monitoring (SHM) after construction. In addition, embedded curing monitoring and a SHM system for high strength concrete can be developed to improve the applicability and efficiency of this system.

6. Acknowledgment

This study was supported by National Nuclear R&D Program through the National Research Foundation of Korea (NRF) funded by the Ministry of Education, Science and Technology (2010-0025889) and u-City Master and Doctor Support Project funded by Ministry of Land, Transport and Maritime Affairs (MLTMA). This all-out support is greatly appreciated.

7. References

ACI Committee 228. (Nov 1, 2003)). *In-place methods to estimate concrete strength report,* American Concrete Institute, MI, USA

Bhalla, S., Naidu, A.S.K. and Soh, C.K. (2002). Influence of structure-actuator interactions and temperature on piezoelectric mechatronic signatures for NDE, *Proceedings of the ISSS-SPIE International Conferences on Smart Materials Structures and Systems*, ISSN 0277786X, Bangalore, December 2002.

Giurgiutiu, V. (July 1, 2007*). Structural health monitoring: with piezoelectric wafer active sensors*, Elsevier/Academic Press, ISBN 9780120887606, Amsterdam

Grisso, B.L. and Inman, D.J. (2005). Developing an autonomous on-orbit impedance-based SHM system for thermal protection systems, *Proceedings of the 5th Int'l Workshop on Structural Health Monitoring*, Stanford, CA, September.

Irie, H., Yoshida, Y., Sakurada, Y., and Ito, T. (2008). Non-destructive-testing Methods for Concrete Structures, *NTT Technical Review*. Vol. 6, No. 8, (May 2008), pp. 1-8

Koo, K.Y., Park, S., Lee, J.J. and Yun, C.B. (2009). Automated impedance-based structural health monitoring incorporating effective frequency shift for compensating temperature effects, *Journal of Intelligent Material Systems and Structures*, Vol. 20, No. 4, pp.367- 377, ISSN 1045389X

Lamond, J. F. and Pielert, J. H. (2006). Significance of tests and properties of concrete and concrete-making materials, *ASTM International*, Vol. 169, pp. 667, ISSN 00660558

Lee, S.J., and Sohn, H. (2006). Active self-sensing scheme development for structural health monitoring, *Smart Materials and Structures*, Vol. 15, No. 6, pp. 1734-1746, ISSN 09641726

Liang, C., Sun, F.P. and Rogers, C.A. (1996). Electro-mechanical impedance modeling of active material systems, *Smart Materials and Structures*, Vol. 5, No. 2, pp. 171-186, ISSN 09641726

Lynch, J.P., Sundararajan, A., Law, K.H., Sohn, H. and Farrar, C.R. (2004). Design of a wireless active sensing unit for structural health monitoring, *Proceedings of the SPIE Annual Int'l Symposium on Smart Structures and Materials*, ISSN 0277786X, San Diego, CA, March.

Mascarenas, D.L., Todd, M.D., Park, G. and Farrar, C.R. (2007). Development of an impedance-based wireless sensor node for structural health monitoring, *Smart Materials and Structures*, Vol. 16, No. 6, pp. 2137-2145, ISSN 09641726

Mascarenas, D.L., Park, G., Farinholt, K., Todd, M.D. and Farrar, C.R. (2009). A low-power wireless sensing device for remote inspection of bolted joints, *Proceedings of the Institution of Mechanical Engineers, Part G: Journal of Aerospace Engineering*, Vol. 223, No. 5, pp. 565-575, ISSN 09544100

Mehta, P. K. and Monterio, P. J. M. (Sep 30, 2005). *Concrete: microstructure, properties, and materials. 3rd ed.*, McGraw-Hill, ISBN 0071462899, New York,

Min, J., Park, S., Yun, C.-B., and Song, B. (2010). Development of Low-cost Multi-functional Wireless Impedance Sensor Nodes, *Smart Structures and Systems*, Vol. 6, No. 5-6 pp. 689-709

Overly, T.G., Park, G., Farrar, C.R. and Allemang, R.J. (2007). Compact hardware development for structural health monitoring and sensor diagnostics using admittance measurements, *Proceedings of the IMAC-XXV: A Conference & Exposition on Structural Dynamics*, Orlando, FL, February 2007.

Overly, T.G., Park, G., Farinholt, K.M. and Farrar, C.R. (2008). Development of an extremely compact impedance-based wireless sensing device, *Smart Materials and Structures*, Vol. 17, No. 6., 065011, ISSN 09641726

Park, G., Cudney, H. H. and Inman, D. J. (2000), Impedance-based health monitoring of civil structural components, *Journal of Infrastructure and Systems,* Vol. 6, No. 4, pp.153-160, ISSN 10760342

Park, G., Sohn, H., Farrar, C.R. and Inman, D.J. (2003). Overview of piezoelectric impedance-based health monitoring and path forward, *Shock and Vibration Digest*, Vol. 35, No. 6, pp. 451-463, ISSN 05831024

Park, G., Farrar, C.R., Rutherford, A.C. and Robertson, A.N. (2006). Piezoelectric active sensor self-diagnostics using electrical admittance measurements, *Journal of Vibration and Acoustics*, Vol. 128, No. 4, pp. 469-476, ISSN 10489002

Park, S., Ahmad, S., Yun, C.-B., and Roh, Y. (2006). Multiple Crack Detection of Concrete Structures Using Impedance-based Structural Health Monitoring Techniques, *Journal of Experimental Mechanics*, Vol. 46, pp.609-618.

Park, S.,, Kim, J.-W., Lee, C.-G., and Park, S.-K. (2011). Impedance-based Wireless Debonding Condition Monitoring of CFRP Laminated Concrete Structures, *NDT&E International*, Vol. 44, pp. 232-238

Park, S., Shin, H.H. and Yun, C.B. (2009), Wireless impedance sensor nodes for functions of structural damage identification and sensor self-diagnosis, *Smart Materials and Structures*, Vol. 18, No. 5, 055001, ISSN 09641726

Park, S., Yun, C.-B., and Roh, Y. , and Lee, J.-J. (2005). Health monitoring of steel structures using impedance of thickness modes at PZT patches, *Journal of Smart Structures and Systems*, Vol. 1, No. 4, pp.339-353.

Shariq, M., Parasad, J. and Masood, A. (2010). Effect of GGBFS on time dependent compressive strength of concrete, *Construction and Building Materials,* Vol. 24, No. 8 pp. 1469-1478, ISSN 09500618

Taylor, S.G., Farinholt, K.M., Park, G. and Farrar, C.R. (2009a). Wireless impedance device for electromechanical impedance sensing and low-frequency vibration data acquisition, *Proceedings of the SPIE Annual International Symposium on Sensors and Smart Structures Technologies for Civil, Mechanical, and Aerospace Systems*, ISBN 978-081947552-7, San Diego, CA, March 2009

Talyor, S.G., Farinholt, K.M., Flynn, E.B., Figueiredo, E., Mascarenas, D.L., Moro, E.A., Park, G., Todd, M.D. and Farrar, C.R. (2009b). A mobile-agent-based wireless sensing network for structural monitoring applications, *Measurement Science and Technology*, Vol. 20, No. 4, 045201, ISSN 09570233

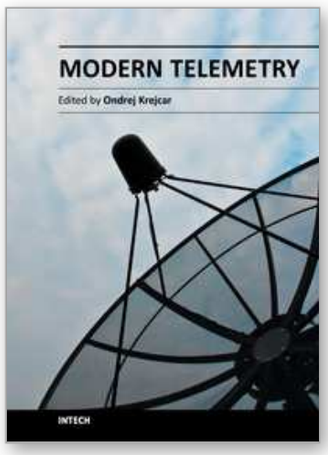

Modern Telemetry
Edited by Dr. Ondrej Krejcar

ISBN 978-953-307-415-3
Hard cover, 470 pages
Publisher InTech
Published online 05, October, 2011
Published in print edition October, 2011

Telemetry is based on knowledge of various disciplines like Electronics, Measurement, Control and Communication along with their combination. This fact leads to a need of studying and understanding of these principles before the usage of Telemetry on selected problem solving. Spending time is however many times returned in form of obtained data or knowledge which telemetry system can provide. Usage of telemetry can be found in many areas from military through biomedical to real medical applications. Modern way to create a wireless sensors remotely connected to central system with artificial intelligence provide many new, sometimes unusual ways to get a knowledge about remote objects behaviour. This book is intended to present some new up to date accesses to telemetry problems solving by use of new sensors conceptions, new wireless transfer or communication techniques, data collection or processing techniques as well as several real use case scenarios describing model examples. Most of book chapters deals with many real cases of telemetry issues which can be used as a cookbooks for your own telemetry related problems.

How to reference
In order to correctly reference this scholarly work, feel free to copy and paste the following:

Seunghee Park and Dong-Jin Kim (2011). Ubiquitous Piezoelectric Sensor Network (UPSN)-Based Concrete Curing Monitoring for u-Construction, Modern Telemetry, Dr. Ondrej Krejcar (Ed.), ISBN: 978-953-307-415-3, InTech, Available from: http://www.intechopen.com/books/modern-telemetry/ubiquitous-piezoelectric-sensor-network-upsn-based-concrete-curing-monitoring-for-u-construction

INTECH
open science | open minds

InTech Europe
University Campus STeP Ri
Slavka Krautzeka 83/A
51000 Rijeka, Croatia
Phone: +385 (51) 770 447
Fax: +385 (51) 686 166
www.intechopen.com

InTech China
Unit 405, Office Block, Hotel Equatorial Shanghai
No.65, Yan An Road (West), Shanghai, 200040, China
中国上海市延安西路65号上海国际贵都大饭店办公楼405单元
Phone: +86-21-62489820
Fax: +86-21-62489821

IntechOpen